Extreme nonlinear optical enhancement in chalcogenide glass fibers with deep-subwavelength metallic nanowires

Bora Ung* and Maksim Skorobogatiy

Department of Engineering Physics, Ecole Polytechnique de Montreal, C. P. 6079, succ. Centre-ville, Montréal, Canada, H3C 3A7

**Corresponding author: boraung@gmail.com*

Received March 23, 2011; revised May 25, 2011; accepted June 7, 2011; posted June 8, 2011 (Doc. ID 144655); published June 29, 2011

A nanostructured chalcogenide–metal optical fiber is proposed. This hybrid nanofiber is embedded with a periodic array of triangular-shaped deep-subwavelength metallic nanowires set up in a bowtie configuration. Our simulations show that the proposed nanostructured fiber supports a guided plasmonic mode enabling both subwavelength field confinement and extreme nonlinear light–matter interactions, much larger than a bare chalcogenide nanowire of comparable diameter. This is all achieved with less than 3% by volume of metal content.

OCIS codes: 060.2390, 060.4005, 190.4370, 240.6680, 250.5403, 230.7370.

In the last decade, different types of photonic crystal fibers and microstructured optical fibers have demonstrated exceptional control over the group velocity chromatic dispersion (GVD) [1]. More recently, advances in micro and nanofabrication techniques have sparked vigorous research on microstructured optical fibers with subwavelength features and using high-refractive-index compound glasses. These so-called emerging waveguides allow the exploration of new operation regimes where tight field confinement, enhanced light–matter nonlinear interactions, and dispersion engineering combine to enable long interaction lengths inside nonlinear media [2]. In parallel, the merging of plasmonics with integrated optics has shown vast potential for sensing [3] and the transmission [4,5] and modulation of optical signals on the subwavelength scale [6–8]. Light guiding mediated by metallic nanowire arrays in optical fibers was also investigated [9–12], and their potential for nonlinear plasmonics was mentioned in [9] but not studied in detail.

In this Letter, we present a new type of nonlinear metallodielectric nanostructured optical fiber (NOF): the chalcogenide fiber with deep-subwavelength metallic inclusions. We demonstrate that the extreme field intensities, obtained at the sharp edges of the subwavelength metallic nanowires, enable giant nonlinear optical enhancements to be achieved inside the hybrid chalcogenide–metal structure. We show that modal propagation losses are comparable to that of classical surface plasmons polaritons (SPPs) and thus only limited by the intrinsic absorption losses of the metal.

When fabricating a fiber comprising several dielectric rods (or capillaries) using the stack-and-draw procedure, the empty interstitial holes [Figs. 1(a) and 1(b)] that may occur between adjacent rods are usually treated as unwanted defects. Here we fill these nanovoids with metal such that we obtain a periodic array of triangle-shaped metallic nanowires, with an orientation akin to so-called "bowtie" nanoantennas [13]. Coincidentally, the bowtie configuration is known to be very effective for yielding strong field confinement inside the nanogap between two opposing apexes [13]. In the proposed fiber design, the intense local fields enabled by metallic bowtie nanowires enhance the nonlinear light–matter interaction within the chalcogenide glass matrix [Figs. 1(c) and 1(d)].

Toward the fabrication of metal (or chalcogenide) nanowires embedded in a dielectric matrix, a practical method was recently demonstrated in [14], where the authors used a consecutive stack-and-draw technique to produce nanowires with extreme aspect ratios. A potential fabrication strategy of this NOF is to first stack identical circular glass rods in a triangular lattice configuration in the preform, and then allow the rods to overlap

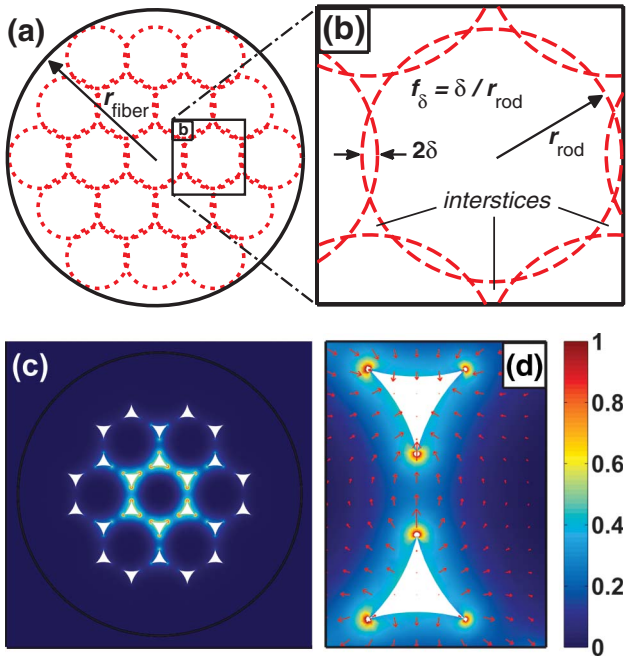

Fig. 1. (Color online) (a) Configuration of overlapping rods and interstices with (b) close-up view of the geometry. (c) S_z-flux distribution of the fundamental plasmonic mode in the chalcometallic nanostructured fiber ($r_{\text{fiber}} = 0.450\,\mu$m, $f_\delta = 0.03$) at $\lambda = 3.0\,\mu$m, and (d) close-up view of the enhanced local fields (arrows denote vector E-fields) in a bowtie pair of nanowires.

during the thermal softening and drawing process. The ensuing small air interstices are then filled by pumping molten metal at high pressure, as demonstrated in [9]. This interstice-filling approach allows the desirable edge-to-edge alignment of pairs of nanowires to be enforced right from the initial macroscopic preform. The wavelength of interest in the present study is $\lambda = 3.0\,\mu$m, at which the permittivity of the gold metal is $-4.74 \times 10^2 + 30.64i$ and its nonlinear index was set to $n_2 = 1.32 \times 10^{-12}\,\mathrm{m^2/W}$ [15]. The chosen dielectric material is As_2Se_3 chalcogenide glass due to its wide bulk transmission window in the mid-IR (2–14 μm) and its large nonlinearity: $n_2 = 1.1 \times 10^{-17}\,\mathrm{m^2/W}$.

To simplify the analysis, the present investigation focuses on the case of $N = 2$ layers of rods (of equal radii r_{rod}) with gold-filled interstices. Nevertheless, the results and discussion presented thereafter provide the foundation for more complex chalcometallic fibers ($N > 2$). In our model, the overlapping of rods is tuned by the "overlap half-distance" δ as defined in Fig. 1(b), and, in practice, this is accomplished by controlling the injected gas pressure when drawing the fiber. Here, we use the non-dimensional parameter $f_\delta = \delta / r_{\mathrm{rod}}$, where $f_\delta = 0$ defines the case of tangent circles; while positive values $0 < f_\delta < f_{\delta,\max}$ controls the overlapping of adjacent rods up to a maximal ratio $f_{\delta,\max} = 0.1339$ (i.e., the limit where the area of the triangular interstice disappears). The total outer radius of the fiber is set to $r_{\mathrm{fiber}} = 5r_{\mathrm{rod}} - 3\delta$ such that the whole geometry can be specified using only r_{fiber} and the "overlap factor" (f_δ), which was kept fixed at 0.03 in this study, corresponding to 2.8% by volume of metal content.

Recently, there have been demonstrations of large nonlinear optical enhancement in chalcogenide nanowires [16]. Therefore, as a benchmark, we compare the optical properties of our hybrid NOF with the bare nanowire (i.e., rod in air). Using full-vector finite-element simulations, we solved for the fundamental HE_{11} mode guided in the bare As_2Se_3 nanowire and for the fundamental plasmonic mode [Fig. 1(c)] guided in the metallo-dielectric NOF at various values of fiber radius. By comparing the bare nanowire with a hybrid NOF of the same size ($r_{\mathrm{fiber}} = 0.32\,\mu$m), one can appreciate the exceptionally strong transverse field confinement in chalcometallic fibers [left inset in Fig. 2(a)], while, in the nanowire case, there is very significant power leakage into the surroundings [right inset in Fig. 2(a)]. Figure 2(b) plots the effective mode area ($A_{\mathrm{eff}} = |\int_{\mathrm{total}} S_z \mathrm{d}A|^2 / \int_{\mathrm{total}} |S_z|^2 \mathrm{d}A$, where $S_z = (\boldsymbol{E} \times \boldsymbol{H}) \cdot \hat{z}$), which indicates that the chalcometallic fiber, consistently provides better field confinement over a chalcogenide nanowire of the same size. In particular, one achieves a nearly tenfold enhancement in field confinement for $r_{\mathrm{fiber}} \geq 0.415\,\mu$m. For $r_{\mathrm{fiber}} < 0.415\,\mu$m, while the A_{eff} of a bare nanowire diverges to the completely unguided limit ($A_{\mathrm{eff}} \to \infty$ for $r_{\mathrm{fiber}} \to 0$), the mode area supported by a chalcometallic fiber keeps shrinking with smaller radii of fiber. This nanoscale localization of light beyond the diffraction limit is made possible by the plasmonic guiding in the metallic nanowire array.

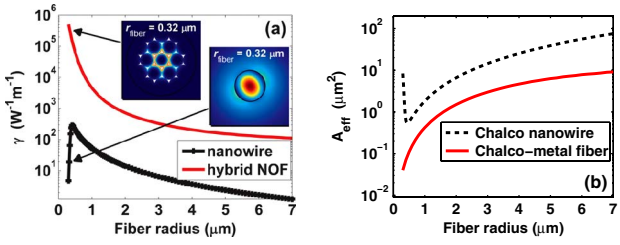

Fig. 2. (Color online) (a) Optical nonlinearity (γ) and (b) effective mode area (A_{eff}) of a bare chalcogenide nanowire and a chalcometallic nanofiber at $\lambda = 3.0\,\mu$m as a function of the fiber radius.

The nonlinear parameter was computed using its vectorial definition [17]:

$$\gamma = \frac{\varepsilon_0}{\mu_0} \cdot \frac{\omega}{c} \cdot \frac{\int_{\mathrm{total}} n^2(x,y) \cdot n_2(x,y) \cdot [2|\boldsymbol{E}|^4 + |\boldsymbol{E}^2|^2] \cdot \mathrm{d}A}{3\left|\int_{\mathrm{total}} S_z \cdot \mathrm{d}A\right|^2}. \tag{1}$$

The full-vector calculations indicate that the hybrid As_2Se_3–gold NOF can theoretically yield nonlinearities over $1 \times 10^4\,\mathrm{W^{-1}m^{-1}}$ at $\lambda = 3.0\,\mu$m [Fig. 2(a)]. In particular, the nonlinearity reaches a peak of $\gamma = 286\,\mathrm{W^{-1}m^{-1}}$ at $r_{\mathrm{fiber}} = 0.415\,\mu$m for the bare nanowire, while, at the same radius size, the hybrid NOF provides $\gamma = 1.34 \times 10^5\,\mathrm{W^{-1}m^{-1}}$ corresponding to a nonlinear enhancement factor of 468, over two orders of magnitude increase in nonlinearity at the given operation wavelength. The nonlinear enhancement factor in chalcometallic fibers (compared to similar nanowires) is consistently greater than 50 across the investigated range of fiber radii.

The effective refractive index $\mathrm{Re}(n_{\mathrm{eff}})$ and effective propagation length, $L_{\mathrm{eff}} = c/2\omega \mathrm{Im}(n_{\mathrm{eff}})$, in the chalco nanowire and the hybrid NOF as a function of fiber radius are plotted in Figs. 3(a) and 3(b), respectively.

As shown in the inset in Fig. 3(a), the fraction of guided power of the fundamental mode in the bare nanowire becomes more confined inside the chalcogenide glass matrix (and less in the air cladding) as the radius of the fiber increases. Consequently, we observe in Fig. 3(a) for the nanowire: $n_{\mathrm{eff}} \to n_{\mathrm{bulk}}$ as $r_{\mathrm{fiber}} \to \infty$, where $n_{\mathrm{bulk}} = 2.789$ at $\lambda = 3.0\,\mu$m for As_2Se_3 glass. The reverse is also true in the unguided limit: the value of n_{eff} reaches the refractive index of air cladding such that $n_{\mathrm{eff}} \to n_{\mathrm{air}} =$

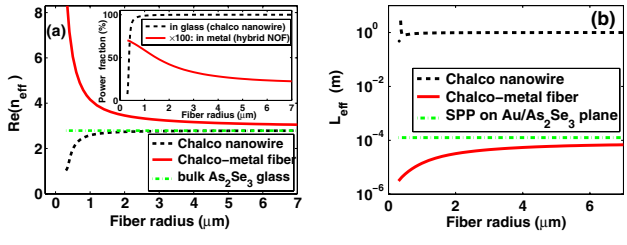

Fig. 3. (Color online) (a) Real effective refractive index (n_{eff}) and (b) effective propagation length (L_{eff}) of a bare chalcogenide nanowire and a chalcometallic nanofiber at $\lambda = 3.0\,\mu$m as a function of the fiber radius. Inset in (a): fraction of power guided inside metallic regions for the chalcometallic fiber (solid curve) and in chalcogenide glass for the nanowire (dashed curve). The n_{eff} and L_{eff} of an SPP on the gold–As_2Se_3 planar interface is shown as a green dot–dashed curve for reference in (a) and (b), respectively.

1 as $r_{\text{fiber}} \to 0$. On the other hand, for the hybrid NOF, the value of n_{eff} increases with reduction of the fiber radius. The latter behavior can be explained by considering the fraction of power that propagates inside metallic regions [solid curve in inset in Fig. 3(a)]. One must first note that the geometrical proportions of the fiber's internal structure are preserved as the radius gets smaller. Hence, for very small NOF radii ($r_{\text{fiber}} < 1\,\mu$m), the dimensions of the metallic nanowires become deeply subwavelength and comparable to the skin depth in metal such that a significant fraction of guided power overlaps with the strongly dispersive metallic regions. The previous remark also explains the gradual lowering of L_{eff} in the hybrid NOF when $r_{\text{fiber}} \to 0$ [Fig. 3(b)]. Figure 3(b) indicates that the effective propagation length of the chalcometallic NOF is comparable in magnitude to that of a planar SPP whose effective index is given by $n_{\text{eff}}^2 = [\varepsilon_m \varepsilon_d/(\varepsilon_m + \varepsilon_d)]$, where ε_m and ε_d denote the dielectric constants of the metal and adjacent dielectric. The latter remark highlights the fact that the guided mode of interest in the metallodielectric NOF is a plasmonic mode created by all the gap-plasmon modes supported by the array of bowtie nanowires. A notable feature here is that a reduction of r_{fiber} from 5.0 to 0.5 μm translates into lowering the L_{eff} value of the hybrid NOF by a factor of 10 [Fig. 3(b)] but at the same time enhancing its nonlinearity 400-fold [Fig. 2(a)]. To alleviate the large plasmonic losses, the incorporation of optical gain via dipolar dopants in the dielectric host (e.g., dye molecules, silicon nanocrystals, and quantum dots) has demonstrated some success [5,18].

The group index, defined as $n_g = n_{\text{eff}} + \omega(dn_{\text{eff}}/d\omega)$, for different values of fiber radius is plotted in Fig. 4(a) as a function of wavelength. We note in Fig. 4(a) that the group index at $\lambda = 3.0\,\mu$m takes values from $n_g = 3.67$ and $n_g = 11.68$ with decreasing fiber size from $r_{\text{fiber}} = 2.25\,\mu$m to $r_{\text{fiber}} = 0.25\,\mu$m. Our simulations indicate that even larger slowdown factors (>20) could be attained at shorter near-IR wavelengths where tighter field confinement is achieved. The GVD was computed using the definition $D = -\lambda/c(d^2 n_{\text{eff}}/d\lambda^2)$. Figure 4(b) shows that via appropriate choice of the geometrical parameters, the chalcometallic NOF enables engineering of the GVD to create a zero-dispersion point (ZDP) at the $\lambda = 3.0\,\mu$m operation wavelength (magenta curve) or even a ZDP at $\lambda = 5.0\,\mu$m along with a flattened dispersion profile (blue curve), thus enabling larger effective bandwidths to be achieved. We also notice some regions where the GVD is engineered to be anomalous, thus allowing nonlinear solitonic effects. Moreover, the ultrafast response (<50 fs) of the third-order nonlinearity in chalcogenide-based waveguides [19] indicates that the proposed NOF can potentially achieve broader bandwidths than all-optical processing devices operating on a resonant-based nonlinearity and without free-carrier effects present in other materials such as silicon. These examples clearly suggest that the proposed hybrid NOF design is not only useful for extreme nonlinear optical interactions but also for slow-light applications with an engineered chromatic dispersion profile.

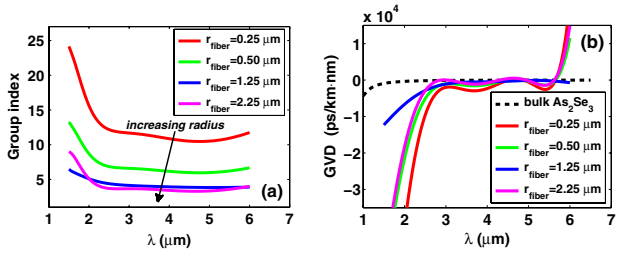

Fig. 4. (Color online) (a) Group index and (b) group velocity dispersion (ps/km/nm) for different values of radius of chalcometallic NOFs as a function of wavelength. In (b), the GVD of bulk As_2Se_3 glass is shown (dashed curve) for reference.

In conclusion, a novel type of NOF is proposed. Our theoretical calculations demonstrate that the hybrid chalcogenide–metal nanofiber provides a platform for achieving nanoscale mode area nonlinear light–matter interactions and also constitutes an alternative path for investigating slow-light applications. Therefore, the proposed chalcometallic fibers are relevant for studying extreme nonlinear light–matter interactions, slow-light guiding systems for all-optical signal processing, and highly integrated nanophotonic devices in general. It also broadens the scope of both conventional and exotic physical phenomena, which can be conveniently studied through the use of micro (nano) structured optical fibers.

References

1. J. M. Dudley and J. R. Taylor, Nat. Photonics **3**, 85 (2009).
2. G. Brambilla, J. Opt. **12**, 043001 (2010).
3. A. Hassani, B. Gauvreau, M. F. Fehri, A. Kabashin, and M. Skorobogatiy, Electromagnetics **28**, 198 (2008).
4. E. Moreno, S. G. Rodrigo, S. I. Bozhevolnyi, L. Martin-Moreno, and F. J. Garcia-Vidal, Phys. Rev. Lett. **100**, 023901 (2008).
5. P. Berini, Adv. Opt. Photon. **1**, 484 (2009).
6. K. F. MacDonald and N. I. Zheludev, Laser Photon. Rev. **4**, 562 (2010).
7. J. A. Schuller, E. S. Barnard, W. Cai, Y. C. Jun, J. S. White, and M. Brongersma, Nat. Mater. **9**, 193 (2010).
8. E. J. Smythe, E. Cubukcu, and F. Capasso, Opt. Express **15**, 7439 (2007).
9. M. A. Schmidt, L. N. Prill Sempere, H. K. Tyagi, C. G. Poulton, and P. St. J. Russell, Phys. Rev. B **77**, 033417 (2008).
10. J. Hou, D. Bird, A. George, S. Maier, B. T. Kuhlmey, and J. C. Knight, Opt. Express **16**, 5983 (2008).
11. A. Manjavacas and F. J. G. Abajo, Opt. Express **17**, 19401 (2009).
12. Z.-X. Zhang, M.-L. Hu, K. T. Chan, and C.-Y. Wang, Opt. Lett. **35**, 3901 (2010).
13. P. J. Schuck, D. P. Fromm, A. Sundaramurthy, G. S. Kino, and W. E. Moerner, Phys. Rev. Lett. **94**, 017402 (2005).
14. A. Mazhorova, J. F. Gu, A. Dupuis, M. Peccianti, O. Tsuneyuki, R. Morandotti, H. Minamide, M. Tang, Y. Wang, H. Ito, and M. Skorobogatiy, Opt. Express **18**, 24632 (2010).
15. P. Wang, Y. Lu, L. Tang, J. Zhang, H. Ming, J. Xie, F.-H. Ho, H.-H. Chang, H.-Y. Lin, and D.-P. Tsai, Opt. Commun. **229**, 425 (2004).
16. C. Baker and M. Rochette, Opt. Express **18**, 12391 (2010).
17. S. Afshar V, W. Q. Zhang, H. Ebendorff-Heidepriem, and T. M. Monro, Opt. Lett. **34**, 3577 (2009).
18. G. Colas des Francs, P. Bramant, J. Grandidier, A. Bouhelier, J.-C. Weeber, and A. Dereux, Opt. Express **18**, 16327 (2010).
19. B. J. Eggleton, B. Luther-Davies, and K. Richardson, Nat. Photonics **5**, 141 (2011).